JET PROPULSION LABORATORY **INTEROFFICE MEMORANDUM**

IOM 312.F – 98 – 048

August 26, 1998

TO : Distribution

FROM : E M Standish

SUBJECT : JPL Planetary and Lunar Ephemerides, DE405/LE405

I. INTRODUCTION

The latest JPL Planetary and Lunar Ephemerides, "DE405/LE405" or just "DE405", have been released and are now available via the Internet or on CDrom (see below) along with the extended and compressed ephemeris, "DE406".

DE405 represents an improvement over its predecessor, DE403, described in detail by Standish *et al.* (1995), and hereafter referred to as the "DE403 Memo". Many of the data sets, reduction techniques, etc. are the same as those used for DE403; they will not be described at length in this memo. Instead, this memo concentrates on the differences: additional data, refinements to the reduction techniques, etc.

The memo discusses the improvement in the orientation of the ephemerides onto the (J2000) International Celestial Reference Frame (ICRF). It shows the increased observational data set used for DE405 and the associated residuals. There is a description of the improved method for modeling the perturbations of asteroids upon the planetary orbits. The individual ephemerides in DE405 are compared with those of DE403. Tables are included of the initial conditions and dynamical constants, resulting from the least squares fitting process and used for the integration.

II. ORIENTATION OF DE405

As has been discussed often, the ephemerides of the four innermost planets along with the moon and the sun are all well-known with respect to each other because of the accurate ranging observations to which the ephemerides are adjusted. In turn, the orientation of this inner system onto the ICRF is also accurately determined, mainly by the VLBI observations of the Magellan Spacecraft orbiting Venus, but also somewhat by VLBI observations of the Phobos Spacecraft approaching Mars, a frame-tie linkage using ground surveys and lunar laser ranging (LLR)data , and the range observations of the Viking Spacecraft on the surface of Mars. Some of the Magellan VLBI observations are new since DE403. These data are discussed in the next section. It is believed that the orientation of the whole inner planet ephemeris system of DE405 is now accurate to about 0.001 arcseconds. A verification of this estimate was provided by the arrival of the Pathfinder Spacecraft at Mars in July 1997, where the ephemeris error was about 0.001 arcseconds, corresponding to 1 km at that distance; it was mostly in the down-track direction.

Ephemerides of the outer planets rely almost entirely upon optical observations; these were initially referenced to various stellar catalogues, then transformed onto the FK4 using the formulae of Schwan (1983), then onto the FK5 system by applying the equinox offset and motion parameters of Fricke (1982), and finally onto the ICRF using tentative transformation tables supplied by Morrison (1996).

III. OBSERVATIONAL DATA

Table I lists the observational data to which DE405 was adjusted. Many of the sets of observational data have been described before (Standish *et al.*, 1976; Standish, 1985, 1990; Standish *et al.*, 1995). Since the creation of DE403, some of these have been augmented by newer data. The actual numbers listed in Table I may differ slightly from those in the DE403 Memo, even though the data set may not have changed. This happens because some of the processing programs automatically eliminate 3-σ values; consequently, a few of the marginal observations may be eliminated from one given ephemeris and not from another.

The observational data fit by the ephemerides are now available over the Internet, as described in Section VIII.

Optical Observations

The basic optical data sets were described in the DE403 Memo. For DE405, new observations, both photoelectric and CCD, of the five outer planets from La Palma, Bordeaux, and USNO Flagstaff Station have been added. The means of the optical residuals for each opposition over the past 20 years are plotted in Figures 1-3, along with error bars indicating the rms value of a single observation.

Since many of the recent optical observations have been referenced to the FK5 frame, as modified by the corrections to precession and equinox drift, it becomes necessary to solve for a difference between the orientation of this frame and that of the ICRF frame. This may be expressed by the formula, $\hat{\mathbf{r}}_{ICRF} \approx \hat{\mathbf{r}}_{FK5} + \mathbf{A} \times \hat{\mathbf{r}}_{FK5}$, where the three components of the vector $\mathbf{A}$ represent small rotations about the x-, y- and z-axes, respectively. However, the determination of the rotation vector $\mathbf{A}$ should not be construed as a significant determination of the FK5-ICRF frame-tie. It is necessary to have both optical and ICRF-based observations of the same planets in order to determine the frame-tie, but in the present case, the optical observations of the inner planets are no longer included in the ephemeris adjustments and there are very few ICRF-based observations of the outer planets. Eventually, it will be best to use an FK5-ICRF frame-tie as determined by other sources; this will be done when such a frame-tie becomes established.

Radar Observations

Radar-ranging observations now exist through 1997 for Mercury, through 1990 for Venus, and through the end of 1994 for Mars. All of the observations since 1982, used for DE405, were taken by the Goldstone 64-m antennae (DSS-14).

In order to account for the topography of Mercury, a set of fully normalized Legendre functions to the second order was adjusted to fit the surface, following Anderson *et al.* (1996):

$$\begin{aligned} R_0 = \quad & +c_{10}\sqrt{3}\sin\phi + (c_{11}\cos\lambda + s_{11}\sin\lambda)\sqrt{3}\cos\phi + c_{20}\tfrac{\sqrt{5}}{2}(3\sin^2\phi - 1) \\ & +(c_{21}\cos\lambda + s_{21}\sin\lambda)\sqrt{15}\sin\phi\cos\phi + (c_{22}\cos 2\lambda + s_{22}\sin 2\lambda)\tfrac{\sqrt{15}}{2}\cos^2\phi \end{aligned}$$

where λ is the longitude and ϕ is the latitude of the echo point on the surface. The least squares adjustment for DE405 yielded

$$\begin{array}{llll} R_0 \equiv 2,439,760m & c_{10} = +920 \pm 523m & c_{11} = +186 \pm 38m & s_{11} = -245 \pm 38m \\ c_{21} = +79 \pm 157m & s_{21} = +744 \pm 166m & c_{22} = +292 \pm 32m & s_{22} = +345 \pm 34m \end{array}$$

It is better to not convert these coefficients into definitive shape parameters for the surface of Mercury, since the whole set of Mercury radar is presently being re-analyzed. Instead, in this context, they have served merely as a smoothing function for determining the Mercury ephemeris.

For Venus, as in DE403, a topographical model of Pettengill *et al.*, (1980), was used to reference the measurements to a sphere whose radius was determined to be 6052.30 ± 0.05 km, in the least squares adjustment.

The residuals for Mercury and Venus are plotted in Figure 4.

For Mars, as in the past, the only radar observations used for DE405 were those used in the closure point analysis. More important for Mars were the spacecraft measurements, described next.

Mars Spacecraft Data

DE405 was fit to 1257 ranging measurements from the Deep Space Network to the Viking Lander Spacecraft on the surface of Mars, 1976-82, and to 629 ranging measurements to the Mariner 9 Spacecraft in orbit around Mars, 1971–72. These are the same data as those used for DE403.

Since the creation of DE405, the following data sets have been received and added to the ephemeris data collection: 14789 Viking doppler points, 89 range points to the landed Pathfinder Spacecraft, and 7564 Pathfinder doppler points. The subsequent adjustments to these data are described by Folkner *et al.* (1997)whose report is recommended for values of parameters describing the rotation and orientation of Mars.

VLBI and Radiometric Observations of Spacecraft

Eight additional VLBI measurements of the Magellan Spacecraft orbiting Venus, taken between May and August 1994, were added since the creation of DE403; all 18 of the Magellan VLBI measurements are plotted in Figure 5. These additional observations have further improved the orientation of DE405 onto the International Celestial Reference Frame (ICRF).

Lunar Laser Ranging Data

Additional LLR ranging data have been received from the MacDonald Laser Ranging Station in Fort Davis, Texas and from the Centre d'Etudes en Recherche en Geodesie et Astronomie (CERGA) in Grasse, France. There are now 11218 normal points from 1970 to 1997; those of the last few years have accuracies of 2-3 cm.

Jupiter Residuals

The frame-tie for Jupiter is provided by adjustment to the recent VLBI observations of the Galileo Spacecraft orbiting Jupiter, as well as the VLBI observations and orbit determination of the Ulysses Spacecraft as it flew by Jupiter in 1992, the VLA observations in 1983, the orbit determination adjustments of the Voyager 1 and Galileo Spacecraft, and range determinations of all spacecraft that have been in the vicinity of Jupiter. The residuals are listed in Table II and plotted in Figure 6. Transit observations from La Palma are included, shown by the stars; those of the Washington 6-inch transit, by open squares. The large open circles, left-to-right, represent the determinations from Voyager 1 (1979.2), VLA (1983.3), Ulysses (1992.1), and Galileo (1995.9), respectively. The full set of Galileo VLBI observations is shown in the third plot of Figure 6, where the the Goldstone-Canberra observations are indicated by an "$\times$", and the Goldstone-Madrid observations by a "$+$". These residuals are plotted again in the fourth plot of Figure 6, where both scales have now been expanded. For DE405, only the first 12 Galileo VLBI measurements were included in the fit. However, it is apparent that all observations are fit by DE405 with an accuracy of about 0."01.

As seen in Table II, the Voyager and VLA residuals are at least twice their *a priori* standard deviation and they remain unexplained. Since the other accurate measurements, Ulysses and Galileo, are well-fit and cover nearly the same parts of the orbit as do the Voyager and VLA measurements, the problem cannot be corrected by a simple adjustment of Jupiter's orbital plane.

There also seem to be signatures in the optical points, some of which are probably attributable to problems in the measurements themselves, as reported by Morrison and Evans (1998) and by Stone (1998). Both noticed that over the past decade, signatures in the Uranus residuals were strikingly similar to signatures in the Neptune residuals, and it is therefore to be assumed that the signatures are caused either by reduction procedures or, since both planets were in the same direction in the sky, zone errors in the catalogues.

IV. MODELING THE ASTEROID PERTURBATIONS

The basic part of the equations of motion for numerically integrating the ephemerides is the same as that described by Newhall *et al.* (1983), and modified as described in the DE403 Memo. Since that time an improved procedure for modeling the asteroids' perturbations upon the earth, moon, and Mars has been used, different from that used for DE403.

The perturbations from the 300 chosen asteroids which significantly affect the planetary and lunar ephemerides are modeled in two different ways:

- the orbits of the "Big3" (Ceres, Pallas and Vesta) were integrated under the gravitational forces of themselves, the sun, planets, and the moon
- these integrated cartesian states of the Big3 were fit with with chebychev polynomials and stored in a temporary file
- the orbits of *non*-Big3 asteroids were integrated under the gravitational forces of the sun, planets, moon and the Big3 asteroids. At each step, the force vectors of these non-Big3 asteroids upon the earth, moon and Mars are computed, summed, and stored in a temporary file. Also stored in the same temporary file were the contributions from these non-Big3 asteroids to the Solar System's center of mass.
- the vectors from this second temporary file were fit with chebychev polynomials and stored in a final file to be used for the full planetary and lunar integration.

The initial conditions and radii of the asteroids came from a file maintained by the Solar System Dynamics Group at JPL. The mass of each individual asteroid was computed from the formula, $GM = 6.27 \times 10^{20}\mathrm{R}^3\rho_k$, where R is the radius of the asteroid in kilometers and where ρ_k is the density of the k^{th} taxonomic class of asteroids (S, C, or M).

The DE405 masses of Ceres, Pallas, and Vesta, in units of the solar mass, were $4.7 \times 10^{-10}, 1.0 \times 10^{-10}, 1.3 \times 10^{-10}$, found in the least squares adjustment of DE405. These are 6%, 29%, and 13% lower, respectively, than those estimated by Standish and Hellings (1989), but are not significantly different from the DE403 values of $4.64 \times 10^{-10}, 1.05 \times 10^{-10}, and 1.34 \times 10^{-10}$, giving mean densities of the C-, S-, and M-class asteroids of 1.8,2.4, and 5.0, respectively.

V. COMPARISON OF DE405 WITH DE403

Figure 7 shows comparisons of geocentric coordinates of the inner planets and moon between DE405 and DE403. Over the full interval of nearly six centuries, the mean motion differences for the earth and Venus are apparent and amount to about $0.''001$/century. The difference in the tidally induced deceleration of the moon is about $0.''06$/century^2.

For the outer planets, Figure 8 shows that the agreement over the present century is within $0.''1$. The differences in mean motions lead to larger differences in other centuries, indicating the uncertainty of extrapolating those orbits beyond the observational data coverage.

Over the time-span of the two ephemerides, 1600 AD to 2200 AD, the heliocentric coordinates of the Earth-Moon Barycenter in DE403 and DE405 may be related quite closely as

$$\hat{\mathbf{r}}_{\mathrm{DE405}} \approx \hat{\mathbf{r}}_{\mathrm{DE403}} + \mathbf{A}(\mathrm{t}) \times \hat{\mathbf{r}}_{\mathrm{DE403}} \quad \text{and} \quad \hat{\mathbf{h}}_{\mathrm{DE405}} \approx \hat{\mathbf{h}}_{\mathrm{DE403}} + \mathbf{A}(\mathrm{t}) \times \hat{\mathbf{h}}_{\mathrm{DE403}}$$

where

$$206265\ \mathbf{A}^T = [\ +0.''0003 - 0.''0002\ T,\quad -0.''0003 + 0.''0001\ T,\quad +0.''0032 - 0.''0009\ T],$$

and where T is the number of centuries past J2000. The three components of the vector **A** represent time-dependent small rotations about the x-, y- and z-axes, respectively.

VI. CONSTANTS, INITIAL CONDITIONS, ETC.

Given in Table III are the dynamical constants used in DE405. Not all of the digits are listed for those constants which are followed by an ellipsis (...). The constants without ellipses are given exactly as they were used in the integration. Their values were found from a preliminary solution, then rounded exactly as shown, and then intorduced into the final solution.

The initial conditions at the starting epoch of the integration, JED 2440400.5 (28 June 1969), are given in Table IV.

VII. DE406, THE NEW "JPL LONG EPHEMERIS"

The full precision numerical integration covered the interval, 3000 BC to 3000 AD. However, only the interval, 1600 AD to 2200 AD, has been fit with full precision chebychev polynomials; this set of polynomials is referred to as DE405. DE406, on the other hand, covers the full interval of the integration, but in order to conserve disk space, lower order chebychev polynomials are used and both the nutations and the lunar librations have been excluded from the file. For DE406, however, the interpolation on the 64-day mesh points remains exact, and for other times, the interpolating accuracy is no worse than 25 meters for all planets and no worse than 1 meter for the moon – adequate for nearly any application except for the processing of the most accurate observations. The nutations may be computed from the formula of the 1980 IAU Nutation Theory, and the librations have been saved on a separate file.

The binary version of DE406 occupies only 3.3 megabytes per century as opposed to the 9.2 required by DE405. For the full expanse, 3000 BC to 3000 AD, DE406 occupies only 200 megabytes.

VIII. AVAILABILITY OF THE EPHEMERIDES AND THE OBSERVATIONS

DE200, DE405, AND DE406

DE200, DE405, and DE406 are available to the general public via anonymous FTP over the Internet or on a CDrom sold by the publisher, Willmann-Bell.

A user is advised to get and read the file, “readme”, available from

- the website, “http://ssd.jpl.nasa.gov” [click on “Horizons” and then click on “DE-200, DE-405, and DE-406”]. , or
- anonymous ftp : “navigator.jpl.nasa.gov” [cd to the directory, “ephem/export”].

As explained in the readme, there are two methods of obtaining the ephemerides themselves:

- anonymous ftp : “navigator.jpl.nasa.gov” [cd to the directory, “ephem/export”].
- from the publisher (≈ $25): Willmann-Bell, Inc.;
  PO Box 35025; Richmond, VA 23235;
  804-320-7016; 804-272-5920 (Fax);
  “http://www.willbell.com/software/jpl.htm”.

The Observational Data Fit by the Ephemerides

The observations being fit by the ephemerides are now available on the website,
“http://ssd.jpl.nasa.gov/plan-eph-data/”.
There are also files describing the formats and giving references to the sources of the data.

IX. CONCLUSION

DE405 represents the most accurate planetary positions available. Certainly, they are not perfect; extrapolation forward or backward in time will always show some amount of deterioration. Subsequent improvements will continue with further acquisition of observational measurements.

X. REFERENCES

Anderson,J.D., Jurgens,R.F., Lau,E.L., Slade,M.A., and Schubert,G.: 1996,“Shape and Orientation of Mercury from Radar Ranging Data”, *Icarus*, **124**, 690–697.

Folkner, W.M., Yoder, C.F., Yuan, D.N., Standish, E.M., and Preston, R.A.: 1997, “Interior Structure and Seasonal Mass Redistribution of Mars from Radio Tracking of Mars Pathfinder”, *Science*, **278**, 1749–52.

Fricke,W.: 1982, "Determination of the Equinox and Equator of the FK5”, *Astron. Astrophys.*, **107**, L13-L16.

Ma, C., Arias, E.F., Eubanks, T.M, Fey, A.L, Gontier, A.-M, Jacobs, C.S., Sovers, O.J., Archinal, B.A., Charlot, P., 1998: “The International Celestial Reference Frame as realized by Very Long Baseline Interferometry”, submitted to *Astron J.*

Morrison, L.V.: 1996, private communication.

Morrison, L.V. and Evans, D.W.: 1998, “Check on JPL DE405 using modern optical observations”, submitted to *Astron Astrophys.*

Newhall, X X, Standish, E.M. and Williams, J.G.: 1983, “DE102: a numerically integrated ephemeris of the Moon and planets spanning forty-four centuries”, *Astron. Astrophys.*, **125**, 150–167.

Pettengill, G.H., Eliason, E., Ford, P.G., Loriot, G.B., Masursky, H., and McGill, G.E.: 1980, "Pioneer Venus Radar Results: Altimetry and Surface Properties", *J. Geophys. Res.*, **85**, A13, 8261–8270; table of values transmitted to the authors via W L Sjogren.

Schwan,H. : 1983, "A Method for the Determination of a System of Positions and Proper Motions of Stars with an Application to the Washington 6 Inch TC Observations", Veroffentlichungen #30, Astronomisches Rechen-Institut, Heidelberg.

Standish,E.M.: 1985, "On the Orientation of Ephemeris Reference Frames", *Cel. Mech. J.*, **37**, 239-242.

Standish,E.M.: 1990, "The observational basis for JPL's DE200, the planetary ephemerides of the Astronomical Almanac", *Astron. Astrophys*, **233**, 252-271.

Standish,E.M., Keesey,M.S.W. and Newhall,X X : 1976, "JPL Development Ephemeris Number 96", Jet Prop Lab Technical Report #32-1603, Pasadena.

Standish, E.M., Newhall, X X, Williams, J.G. and Folkner, W.F.: 1995, "JPL Planetary and Lunar Ephemerides, DE403/LE403", JPL IOM 314.10-127.

Standish, E.M. and Hellings, R.W.: 1989, "A Determination of the Masses of Ceres, Pallas and Vesta from their Perturbations upon the Orbit of Mars", *Icarus*, **80**, 326-333.

Stone, R.C.: 1998, "CCD Positions for the Outer Planets in 1996–1997 Determined in the Extra-galactic Reference Frame", submitted to *Astron J.*.

Table I. Observational data fit by DE405. The columns contain the source, the time coverage, the planets measured, the components measured, the *a priori* uncertainties of a measurement, the number of observations and the group totals.

OPTICAL MERIDIAN TRANSITS						
Washington	1911–1994	Sun, ..., Nep	r.a., dec.	$1''.0/0''.5$	14242	
Herstmonceux	1957–1982	Sun, ..., Nep	r.a., dec.	$1''.0/0''.5$	2851	17093
PHOTOELECTRIC MERIDIAN TRANSITS						
La Palma	1984–1993	Mar, ..., Plu	r.a., dec.	$0''.25$	6410	
Bordeaux	1985–1996	Sat, Ura, Nep	r.a., dec.	$0''.25$	854	
Tokyo	1986–1988	Mar, ..., Nep	r.a., dec.	$0''.5$	498	
Flagstaff - USNO	1995	Plu	r.a., dec.	$0''.1$	20	7782
ASTROLABE						
Quito	1969	Sat	r.a., dec.	$0''.3$–$1''.6$	1	
Algiers	1969–1973	Mar,Sat			48	
SanFernando	1970–1978	Mar,Jup,Sat			338	
Besançon	1971–1973	Sat			44	
Paris	1971–1978	Mar,Sat			146	
CERGA	1972–1981	Mar,Jup,Sat			202	
Santiago	1975–1985	Ura			284	1063
PHOTOGRAPHIC ASTROMETRY OF PLUTO						
(Pre-disc)	1914–1927	Pluto	r.a., dec.	$0''.5$	28	
Lowell	1930–1951				620	
Yerkes-McD	1930–1953				310	
(Nrml pts.)	1930–1958				66	
MacDonald	1949–1953				56	
Yerkes	1962–1963				42	
Palomar	1963–1965				8	
Dyer	1964–1981				44	
Bordeaux	1967				24	
Asiago	1969–1978				350	
Torino	1973–1982				74	
Copenhagen	1975–1978				150	
Flagstaff	1980–1994				16	
Lick	1980–1985				56	
La Silla	1988–1989				58	1902
CCD ASTROMETRY OF URANUS, NEPTUNE AND PLUTO						
Flagstaff - USNO	1995-1996	Ura, Nep	r.a., dec.	$0''.20$	313	
Flagstaff - USNO	1995-1996	Plu	r.a., dec.	$0''.20$	63	
Bordeaux	1995	Plu	r.a., dec.	$0''.20$	13	389

OCCULTATION TIMINGS						
Uranus rings	1977–1983	Ura	r.a., dec.	0″.14	14	
Neptune disk	1968–1985	Nep	r.a., dec.	0″.27	18	32
RADAR RANGING						
Arecibo	1967–1982	Mer,Ven	range	10 km	284	
Haystack	1966–1971	Mer,Ven		1.5	188	
Goldstone13	1964–1970	Ven		1.5	9	
Gldstn 13–14	1970–1977	Mer,Ven		1.5	23	
Goldstone14	1970–1993	Mer,Ven		1.5	376	880
MARS RADAR–RANGING CLOSURE POINTS						
Goldstone14	1971–1993	Mars	diff. range	1.5	65	65
RADIO ASTROMETRY OF THERMAL EMISSION						
VLA	1987	Jup, ..., Nep	r.a., dec.	0″.03–0″.1	10	10
SPACECRAFT MEASUREMENTS						
Mariner 9	1971–1972	Mars	range	35–120 m	629	
Pioneer 10	1973	Jupiter	range	3 km	1	
Pioneer 11	1974			12 km	1	
Viking Lander	1976–1980	Mars	range	7 m	1018	
	1980–1981			12 m	264	
Voyager 1 OD	1979	Jupiter	r.a., dec.	0″.01, 0″.05	2	
			range	3 km	1	
Voyager 2 OD	1979		range	3 km	1	
Phobos OD	1989	Mars	range	0.5 km	1	
Phobos VLBI	1989	Mars	r.a., dec.	0″.01–0″.1	2	
Ulysses VLBI & OD	1992	Jupiter	r.a., dec.	0″.003, 0″.006	2	
			range	3 km	1	
Magellan VLBI	1990–1994	Venus	r.a., dec.	0″.003–0″.01	18	
Galileo OD	1995	Jupiter	r.a., dec.	0″.05, 0″.2	2	
			range	20 km	1	1956
FRAME-TIE DETERMINATION						
ICRF frame-tie	1988	Earth	$\hat{\mathbf{r}}_\oplus$, $\hat{\mathbf{h}}_\oplus$	0″.003	6	6
LUNAR LASER RANGING						
	1969–1996	Moon	range	2–30 cm	11218	11218
NOMINAL VALUES						
					1	1
TOTAL						42410

Table II. Residuals of Jupiter for DE405 in right ascension, declination, and range.

Pioneer 10	4 Dec 1973					−9.1 km	± 3.0 km
Pioneer 11	3 Dec 1974					−7.8 km	± 12.0 km
Voyager 1 OD	5 Mar 1979	$+0\overset{''}{.}044$	$\pm\ 0\overset{''}{.}020$	$+0\overset{''}{.}155$	$\pm\ 0\overset{''}{.}050$	−2.3 km	± 3.0 km
Voyager 2 OD	9 Jul 1979					−4.7 km	± 3.0 km
VLA	Apr/May 1983	$-0\overset{''}{.}025$	$\pm\ 0\overset{''}{.}030$	$-0\overset{''}{.}133$	$\pm\ 0\overset{''}{.}060$		
Ulysses VLBI & OD	8 Feb 1992	$0\overset{''}{.}000$	$\pm\ 0\overset{''}{.}003$	$-0\overset{''}{.}001$	$\pm\ 0\overset{''}{.}006$	−0.7 km	± 3.0 km
Galileo OD	7 Dec 1995	$-0\overset{''}{.}004$	$\pm\ 0\overset{''}{.}003$	$+0\overset{''}{.}006$	$\pm\ 0\overset{''}{.}006$	+6.3 km	± 3.0 km

Table III. Primary constants for DE405

JED SPAN : 2305424.50 (1599 Dec 09) to 2525008.50 (2201 Feb 20)

AU	149597870.691	[km/au]
CLIGHT	299792.458	[km/sec]
EMRAT	81.30056	[GM(earth)/GM(moon)]

	$[\mathrm{au}^3/\mathrm{day}^2]$	$[\mathrm{GM}_{\mathrm{Sun}}$	$/\mathrm{GM}_{\mathrm{i}}]$	$[\mathrm{km}^3/\mathrm{sec}^2]$
GM1	$0.4912547451450812...\times10^{-10}$	6023600	.	22032.080...
GM2	$0.7243452486162703...\times10^{-09}$	408523	.71	324858.599...
GM3	$0.8887692390113509...\times10^{-09}$	332946	.050895...	398600.433...
GM4	$0.9549535105779258...\times10^{-10}$	3098708	.	42828.314...
GM5	$0.2825345909524226...\times10^{-06}$	1047	.3486	126712767.863...
GM6	$0.8459715185680659...\times10^{-07}$	3497	.898	37940626.063...
GM7	$0.1292024916781969...\times10^{-07}$	22902	.98	5794549.007...
GM8	$0.1524358900784276...\times10^{-07}$	19412	.24	6836534.064...
GM9	$0.2188699765425970...\times10^{-11}$	135200000	.	981.601...
GMS	0.01720209895^2	1	.	132712440017.987...
GMM	$0.1093189565989898...\times10^{-10}$	27068700	.387534...	4902.801...
GMB	$0.8997011346712499...\times10^{-09}$	328900	.561400	403503.233...

	$[\mathrm{au}^3/\mathrm{day}^2]$	$[\mathrm{GM}_{\mathrm{i}}$	$/\mathrm{GM}_{\mathrm{Sun}}]$	$[\mathrm{km}^3/\mathrm{sec}^2]$
MA0001	$0.1390787378942278...\times10^{-12}$	4.7	$\times10^{-10}$	62.375...
MA0002	$0.2959122082855911...\times10^{-13}$	1.0	$\times10^{-10}$	13.271...
MA0004	$0.3846858707712684...\times10^{-13}$	1.3	$\times10^{-10}$	17.253...

Table IV. DE405 positions and velocities at the integration epoch. Heliocentric planets, geocentric moon, solar-system-barycentric sun at JED 2440400.5 (June 28, 1969), in au and au/day.

Mercury	0.3572602064472754	−0.0915490424305184	−0.0859810399869404
	0.0033678456621938	0.0248893428422493	0.0129440715867960
Venus	0.6082494331856039	−0.3491324431959005	−0.1955443457854069
	0.0109524201099088	0.0156125067398625	0.0063288764517467
EM-Bary	0.1160149091391665	−0.9266055536403852	−0.4018062776069879
	0.0168116200522023	0.0017431316879820	0.0007559737671361
Mars	−0.1146885824390927	−1.3283665308334880	−0.6061551894193808
	0.0144820048079447	0.0002372854923607	−0.0002837498361024
Jupiter	−5.3842094069921451	−0.8312476561610838	−0.2250947570335498
	0.0010923632912185	−0.0065232941911923	−0.0028230122672194
Saturn	7.8898899338228166	4.5957107269260122	1.5584315167250895
	−0.0032172034910937	0.0043306322335557	0.0019264174637995
Uranus	−18.2699008149782607	−1.1627115802190469	−0.2503695407425549
	0.0002215401656274	−0.0037676535582462	−0.0016532438049224
Neptune	−16.0595450919244627	−23.9429482908794995	−9.4004227803540061
	0.0026431227915766	−0.0015034920807588	−0.0006812710048723
Pluto	−30.4878221121555448	−0.8732454301967293	8.9112969841847551
	0.0003225621959332	−0.0031487479275516	−0.0010801779315937
Moon	−0.0008081773279115	−0.0019946300016204	−0.0010872626608381
	0.0006010848166591	−0.0001674454606152	−0.0000855621449740
Sun	0.0045025081562339	0.0007670747009324	0.0002660568051770
	−0.0000003517482096	0.0000051776253996	0.0000022291018544

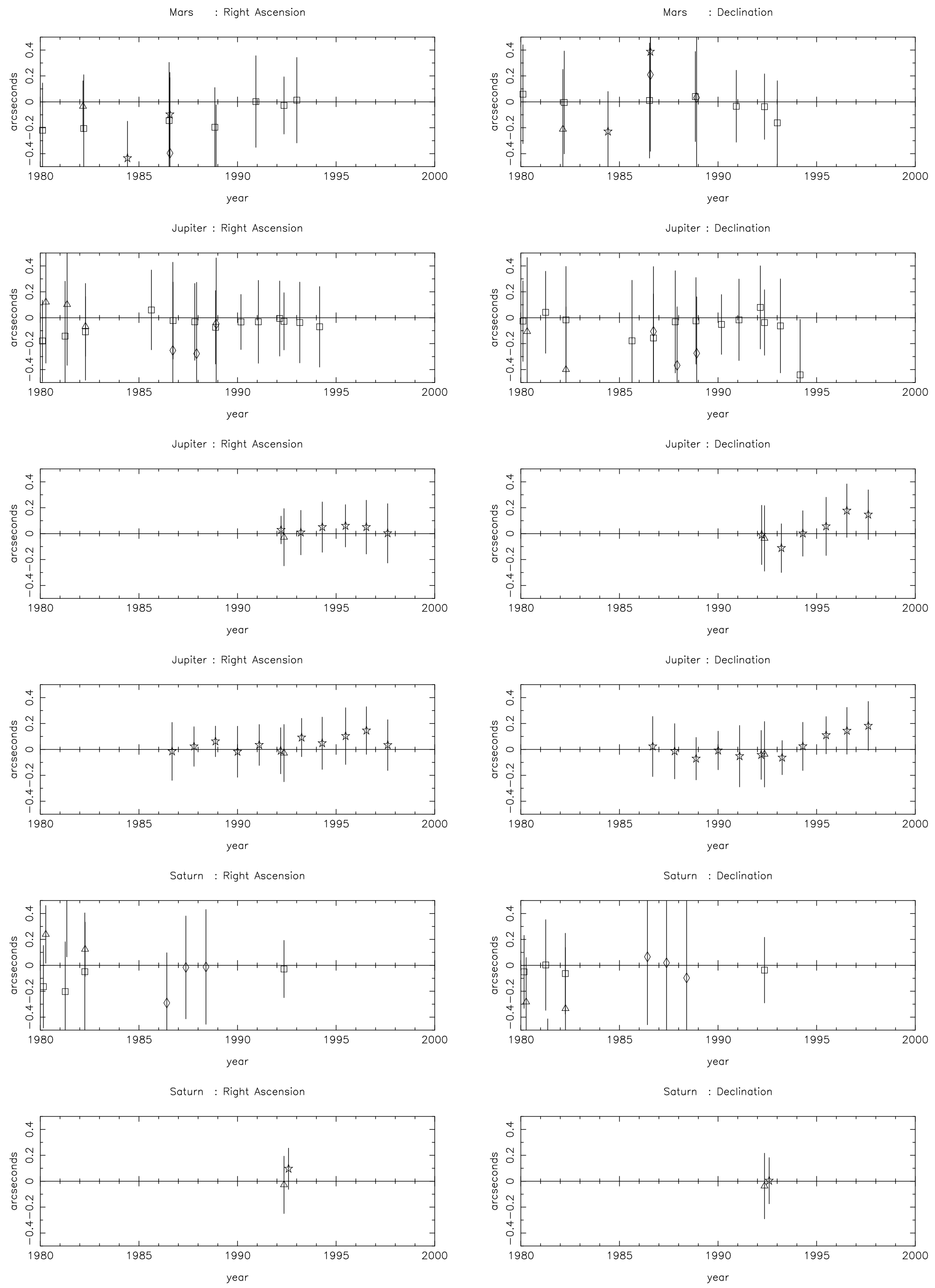

Figure 1: Opposition means of the transit observations: RGO, Herstmonceux (triangles); RGO, La Palma (stars); Bordeaux (circles); USNO, Washington 6-inch (squares); Tokyo (diamonds). The error bars correspond to the rms of a single observation.

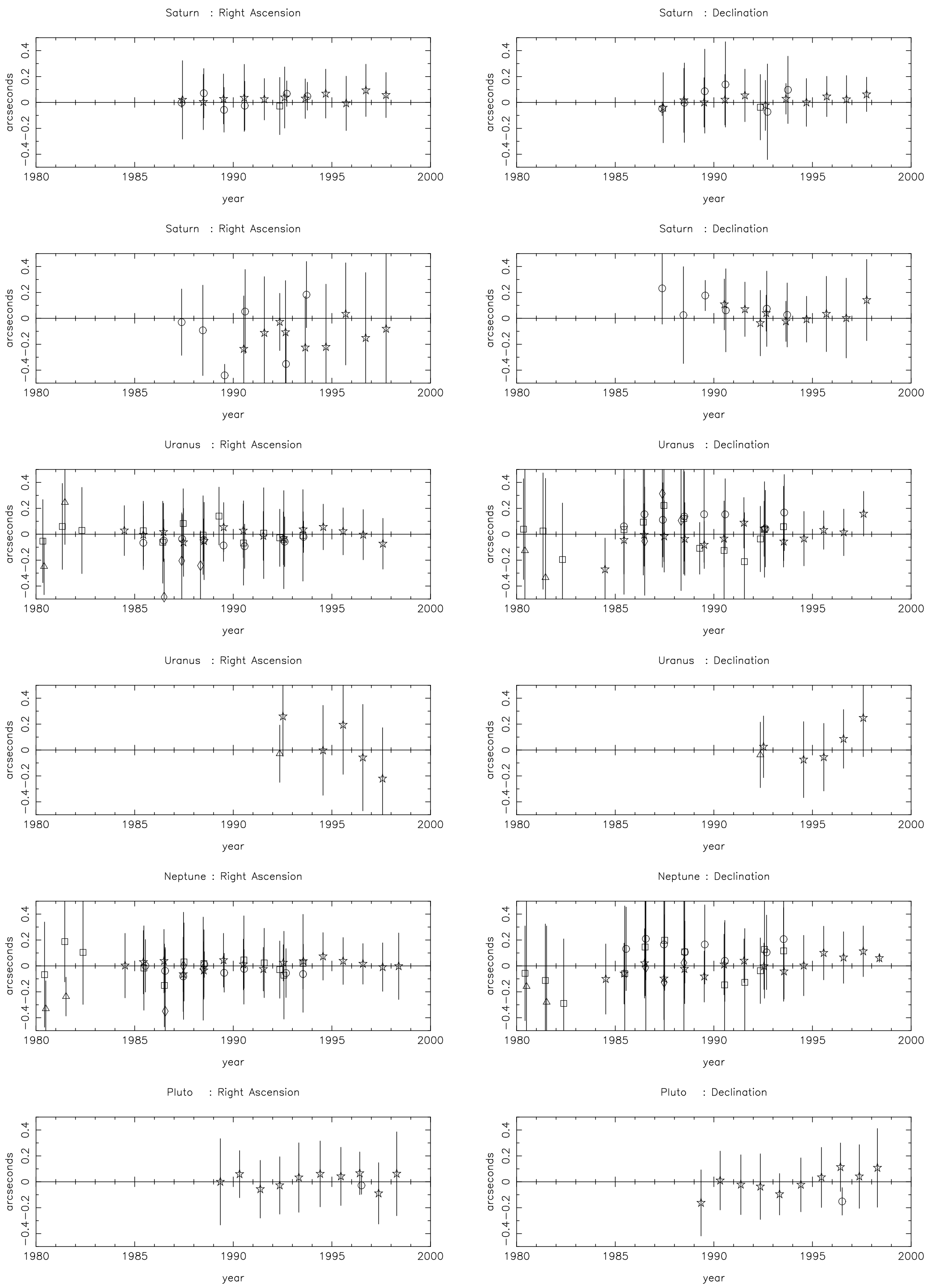

Figure 2: Opposition means of the transit observations (continued from Figure 1).

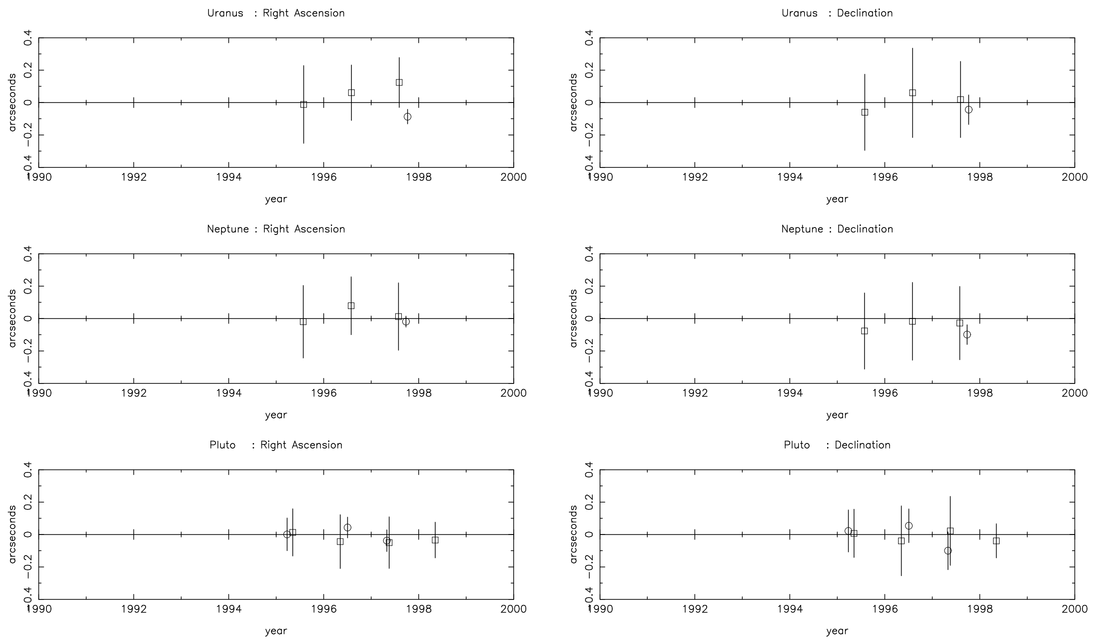

Figure 3: Opposition means of USNO Flagstaff (squares) and of Bordeaux (circles). The error bars correspond to the rms of a single observation.

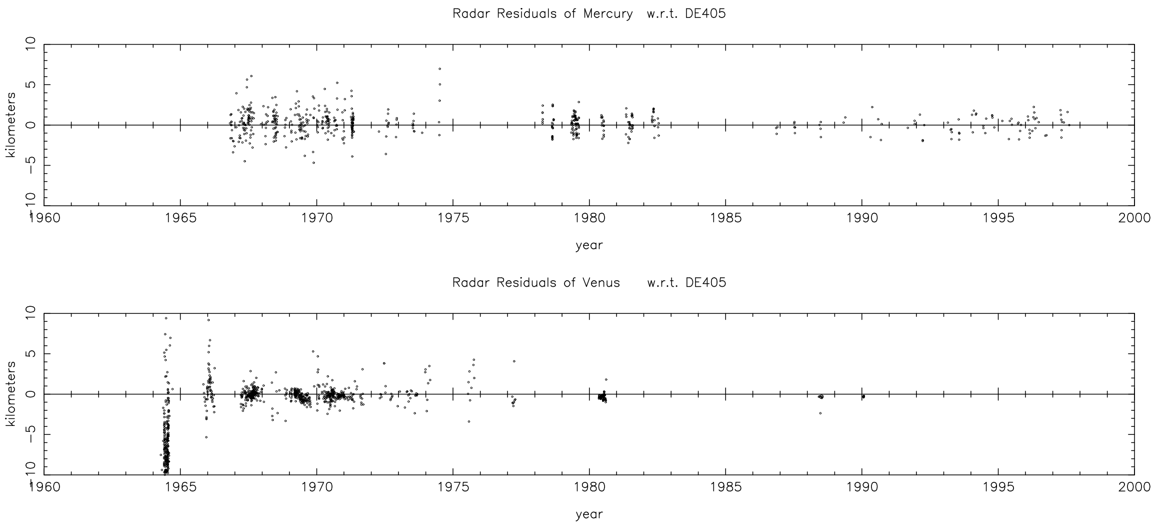

Figure 4: Radar residuals for Mercury and Venus. The early observations have been severely down-weighted.

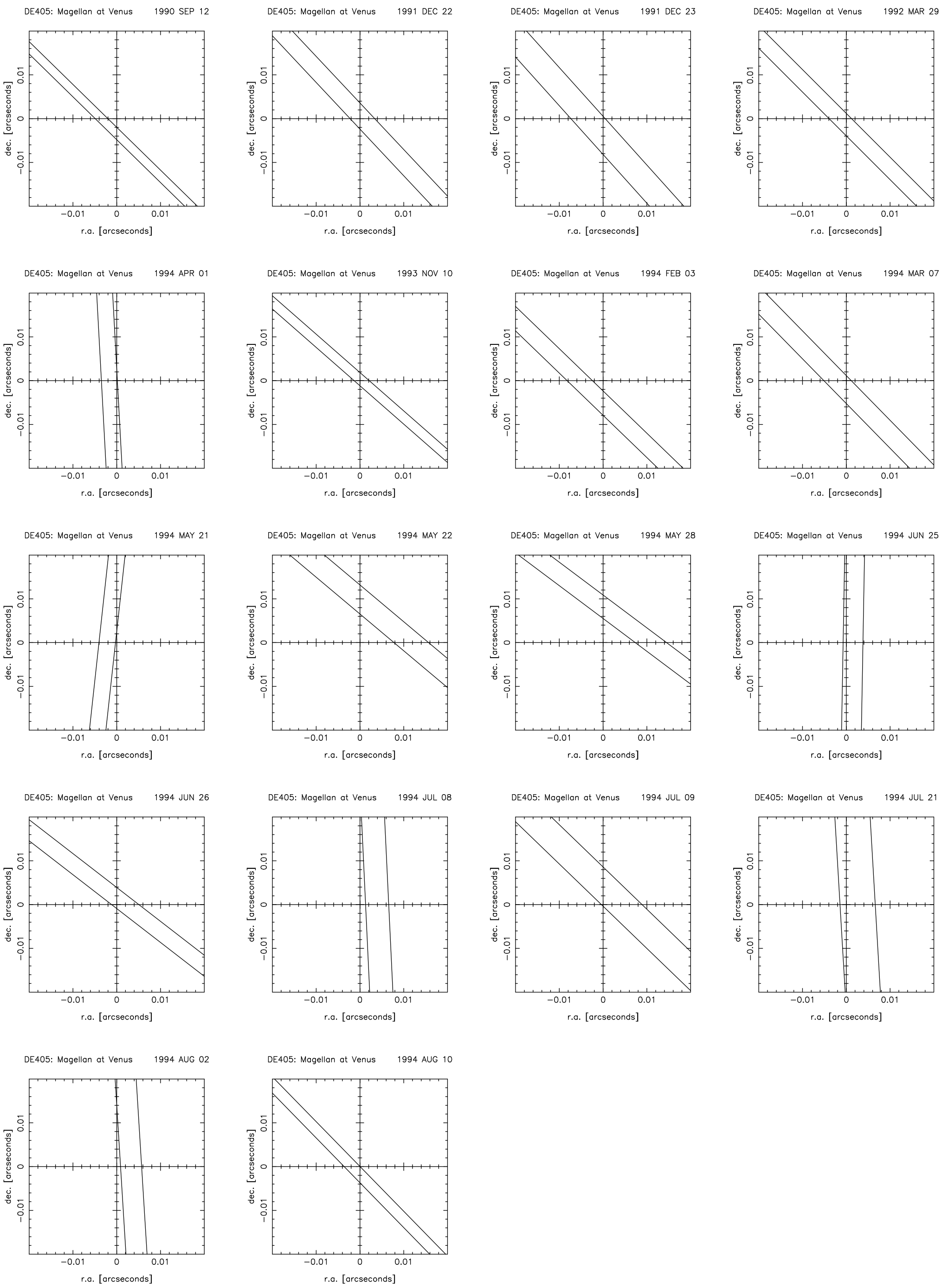

Figure 5: The VLBI residuals of the Magellan Spacecraft orbiting Venus, plotted with right ascension vs. declination. The observations are one-dimensional; the 1-σ lines surrounding the solution line are shown. The Goldstone-Madrid observations are nearly all in right ascension; the Goldstone-Canberra observations are about equally divided between r.a. and dec.

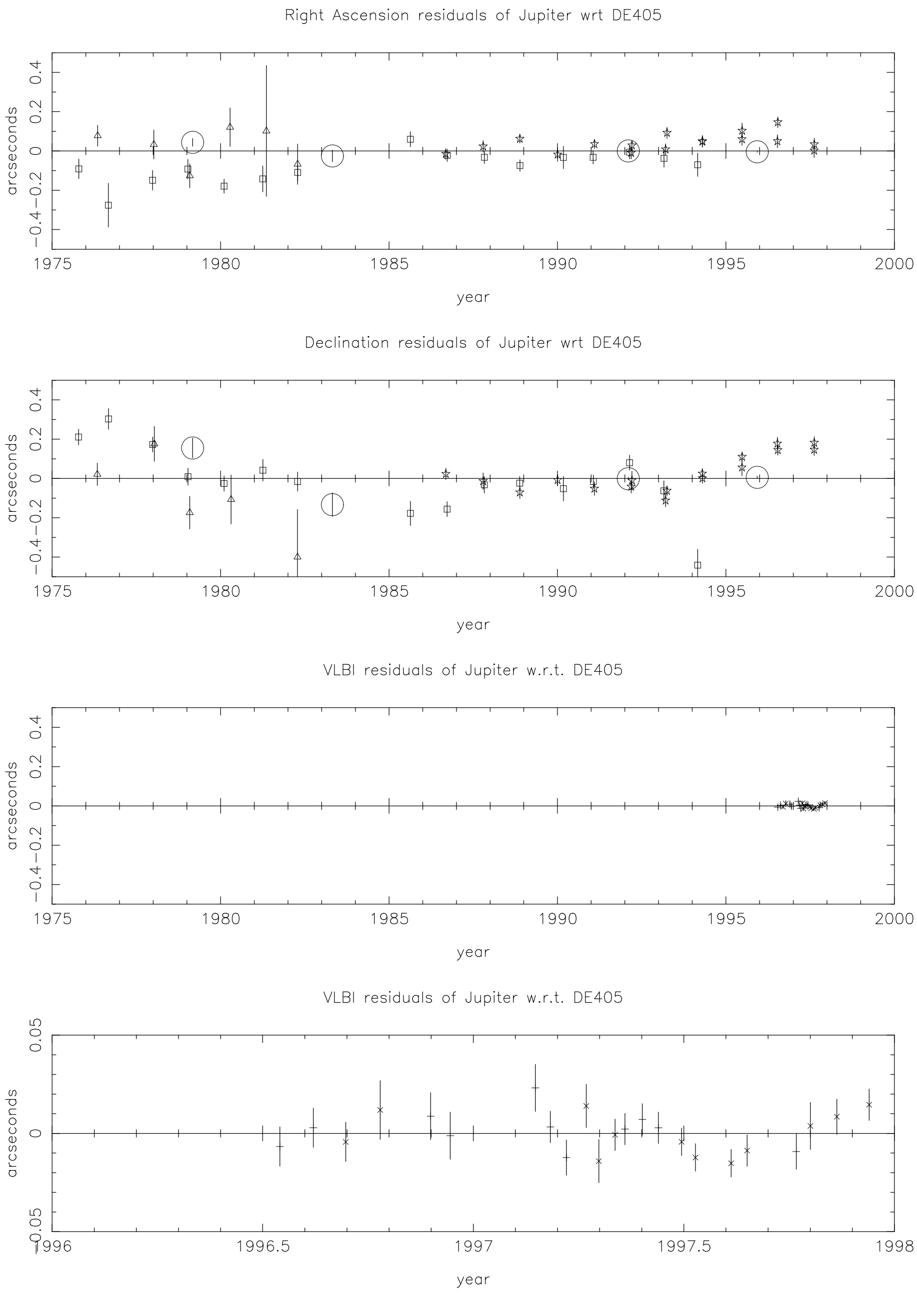

Figure 6: The residuals of Jupiter: The first two plots show right ascension and declination residuals of Jupiter, with the large open circles representing, left-to-right, Voyager 1 (1979.2), VLA (1983.3), Ulysses (1992.1), and Galileo (1995.9), respectively. Also included are opposition means of transit observations from the RGO, Herstmonceux (triangles), from the RGO, La Palma (stars), and from the USNO, Washington 6-inch (open squares). The third plot shows VLBI observations from the Galileo spacecraft: Goldstone-Canberra observations, indicated by an "×" and Goldstone-Madrid observations by a "+". The final plot is identical to the third, except that both the vertical and horizontal scales have be expanded.

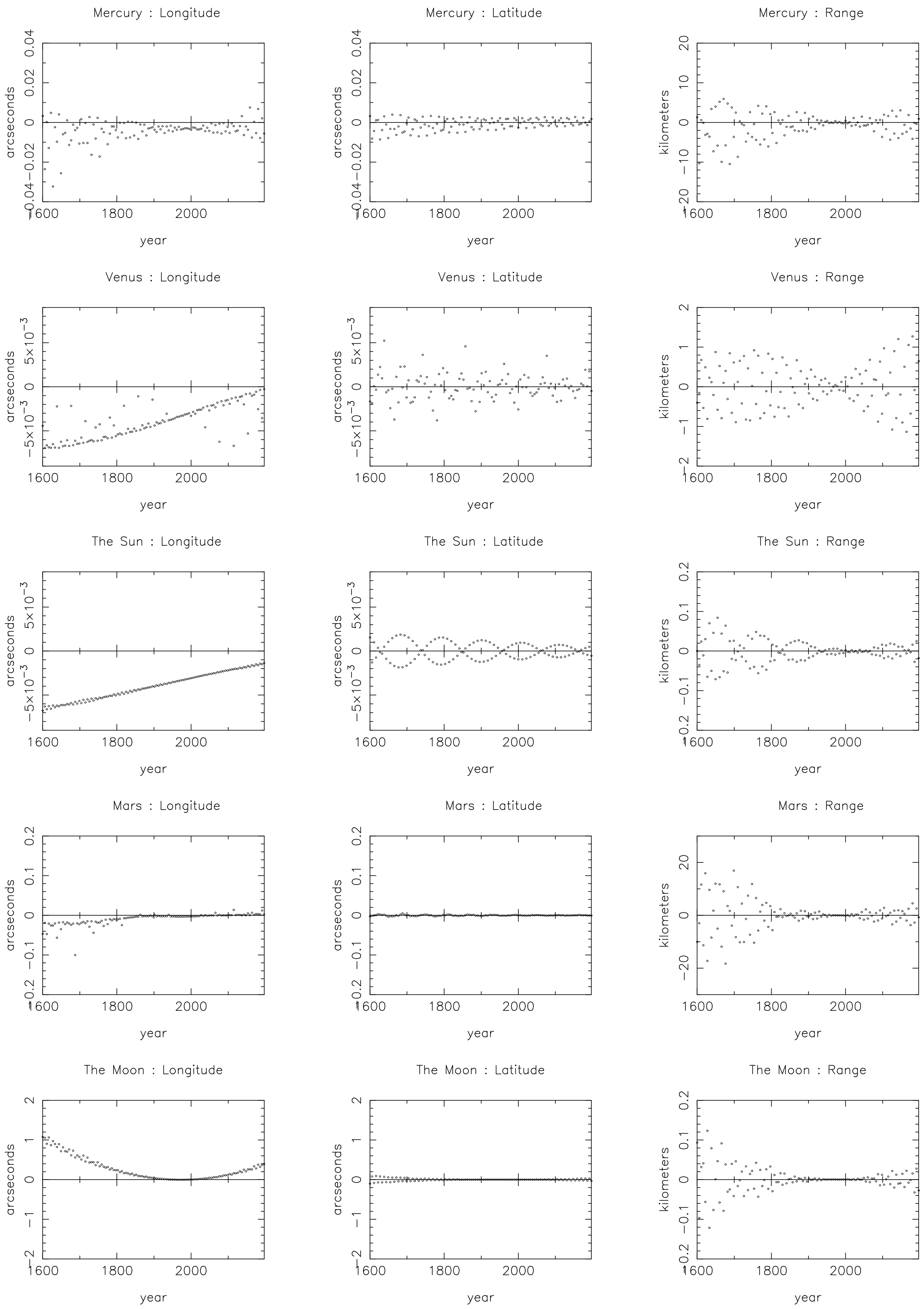

Figure 7: DE403 – DE405 : Geocentric comparisons for the inner planets.

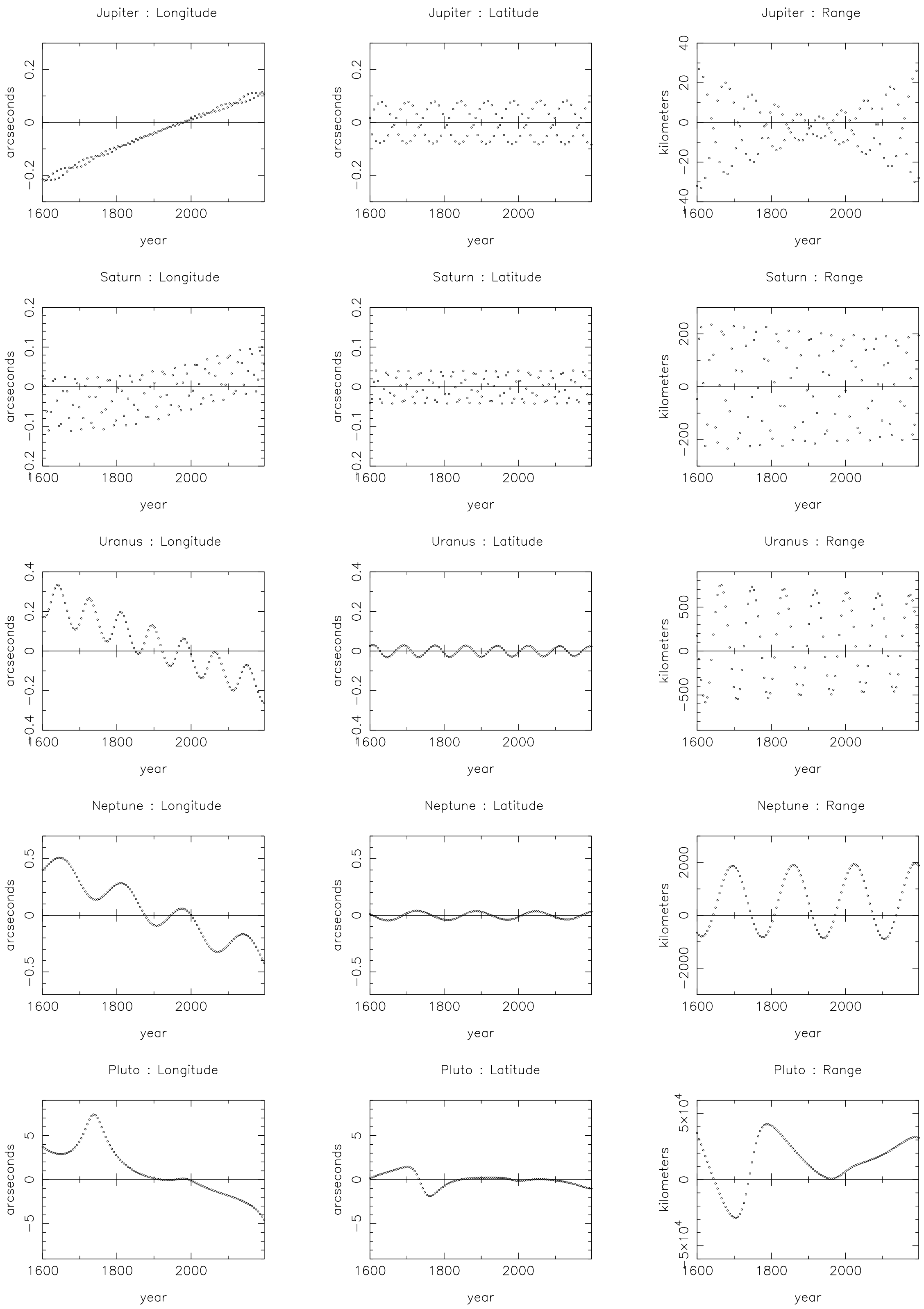

Figure 8: DE403 – DE405 : Heliocentric comparisons for the outer planets.